# Multi Subband Deterministic Simulation of an Ultra-thin Double Gate MOSFET with 2D Electron Gas

Tiao Lu[a,†], Gang Du[b], Haiyan Jiang[c], Xiaoyan Liu[b], Pingwen Zhang[a]
a) School of Mathematical Sciences, LAMA and CAPT, Peking University, Beijing 1000871, China
b) Institute of Microelectronics, Peking University, Beijing, 100871, China
c) Department of Applied Mathematics, Beijing Institute of Technology, Beijing 100081, China
† tlu@math.pku.edu.cn

***Abstract*—We present a self-consistent multi subband deterministic solver of the Boltzmann transport equation of the two dimensional (2D) electron gas. The Schödinger equation at each slice in the confinement direction and the two dimensional Poisson equation are self-consistently solved with the Boltzmann transport equation. The energy quantization and the scattering of the 2D electron gas are included. We apply this solver to an ultra-thin body double gate MOSFET and show the influence of the 2D$k$ scattering to the electron transport.**

***Index Terms*—Double Gate MOSFET, Multi subband deterministic solver, transport, 2D Electron Gas**

## I. INTRODUCTION

The Double Gate (DG) MOSFET is a structure for ultimate scaling since the second gate electrode can overcome the short channel effects in a nano-scale MOSFET [1]. The simulation of Ultra-thin body DG MOSFETs has drawn the interest of many researchers [2]–[4]. For such a structure, the electrons can still be treated semi-classically in the transport direction (source-to-drain direction), but the scattering effects can not be ignored. Due to the ultra thin body, the energy quantization influences the property of the device greatly. In order to include the vertical quantum effects, the energy quantization and the 2D$k$ scattering, which is more appropriate than the free electron scattering (3D$k$ scattering), need to be properly included [2].

Until now, only Monte Carlo methods have been used for such a multi subband model with the 2D$k$ scattering. But it is well known that a deterministic solver for the BTE has many advantages over Monte Carlo methods in many situations, especially for the low dimensional transport [5]. The deterministic solver for the BTE has been used to investigate the Boltzmann-Poisson system [6] but has not been used to investigate the multi subband model with 2D$k$ scattering. We propose a finite volume method based on the characteristic curve method for the time dependent multi subband BTE with low dimensional (2D$k$) scattering. It is the first time a deterministic multi subband model simulator with 2D$k$ scattering is presented. We apply our code to a nano scale DG MOSFET and show the influence of the 2D$k$ scattering to the electron transport.

## II. METHODOLOGY

A DG MOSFET is illustrated in Fig. 1. We use a model similar to that in [2], [7]. The electrons are confined in two gate

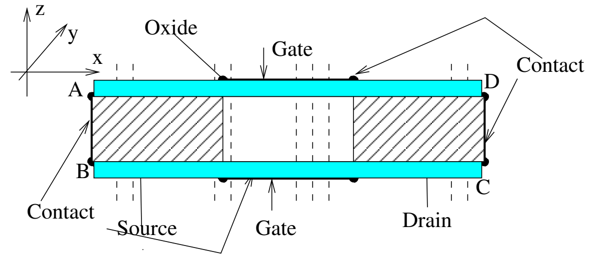


Fig. 1. Schematic of the ultra-thin body DG MOSFET structure

stacks, and a Schrödinger equation along the vertical direction ($z$-direction)

$$\left[-\hbar^2 \frac{d}{dz}\left(\frac{1}{2m_{z,i}}\frac{d}{dz}\right) + V(x,z)\right]\varphi_i(z;x) = E_i(x)\varphi_i(z;x) \tag{1}$$

at each $x$-slice is solved to include the quantum confinement effect where $m_{z,i}$ is the effective mass of the electron on the subband $i$ in the $z$-direction and $V(x,z)$ is the potential. $E_i(x)$ is the eigen energies and $\varphi_i(z;x)$ is the eigen wavefunctions where the subbands are numbered by $i$. We choose the six ellipsoidal parabolic $\Delta$ valleys, and $m_{z,i}$ is equal to the transverse effective mass $m_t = 0.19m_0$ or the longitudinal effective mass $m_l = 0.916m_0$, where $m_0$ is the free electron rest mass.

The movement of the electrons on each subband from source to drain are modelled by the multi subband semi-classical BTE

$$\frac{\partial f_i}{\partial t} + v_{x,i}\frac{\partial f_i}{\partial x} + \frac{F_i(x)}{\hbar}\frac{\partial f_i}{\partial k_x} = \left.\frac{\partial f_i}{\partial t}\right|_{scat}. \tag{2}$$

where $f_i = f_i(t,x,k_x,k_y)$ is the distribution function for the electrons on the $i$-th subband, and $v_{x,i}$ is the velocity of the $i$-th subband's electrons in the $x$-direction. According to the mode space approach, the electric force $F_i(x)$ on each subband along the transport direction ($x$-direction) is related to the derivative of the associated energy $E_i(x)$, $F_i(x) = -\frac{dE_i(x)}{dx}$.

The initial distribution functions of each subband are given by the Fermi-Dirac distribution

$$f_i(t=0,x,k_x,k_y) = \frac{1}{1+e^{\frac{E_i(x)+\omega(k_x,k_y)-\mu(x)}{k_BT}}} \tag{3}$$

978-1-4244-3927-0/09/$25.00 ©2009 IEEE



Authorized licensed use limited to: Peking University. Downloaded on December 17, 2009 at 04:34 from IEEE Xplore. Restrictions apply.

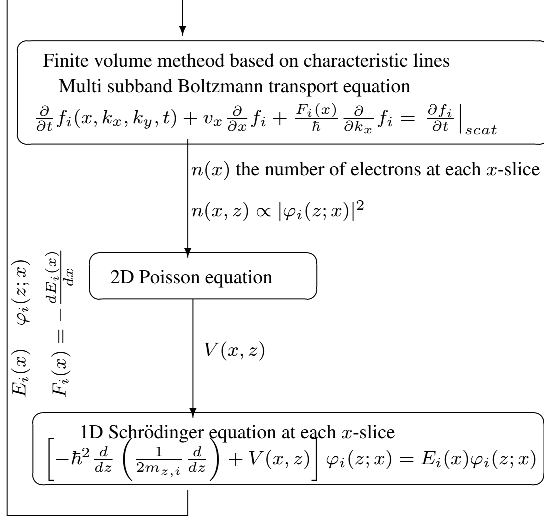


Fig. 2. A deterministic solver for the multi subband BTE in one time step

where $\omega(k_x, k_y) = \frac{\hbar^2 k_x^2}{2m_{x,i}} + \frac{\hbar^2 k_y^2}{2m_{y,i}}$ and $m_{x,i}$ and $m_{y,i}$ are the effective masses of the electrons on the subband $i$ in the $x$-direction and $y$-direction in $\mathbf{k}$ space respectively; $\mu(x)$ is the quasi Fermi level. Here $E_i(x)$ is obtained by solving the self-consistent Schrödinger-Poisson system [1]. Both the inter-valley and intra-valley scattering between 2D electron gas and phonons are considered.

During each time step, the multi subband BTE of 2D electron gas solved by the deterministic solver is illustrated in Fig. 2. The deterministic solver we use is the finite volume method based on the analysis of the characteristic curves. First we use a change of variables

$$k_x = \frac{\sqrt{m_{x,i}}}{\hbar}\sqrt{2\omega}\cos\theta, \quad k_y = \frac{\sqrt{m_{y,i}}}{\hbar}\sqrt{2\omega}\sin\theta \qquad (4)$$

in order to facilitate accurate integration of $\delta$ functions in the scattering term. $f_i(t, x, \omega, \theta)$ is sampled as the volume average of a control volume $\Omega_{j,k,l} = [x_{j-1/2}, x_{j+1/2}] \times [\omega_{l-1/2}, \omega_{l+1/2}] \times [\theta_{l-1/2}, \theta_{l+1/2}]$. The Algorithm 745 is used to do the incomplete Fermi-Dirac integral [8]. Secondly, for the transport part we introduce a finite volume method based on the movement of the surface of the control volume along the characteristic curves. Finally, we use the second order Strang's time splitting technique [9] to solve the BTE with 2D$k$ scattering. Our method can preserve the numerical conservation of the particle number and also handle the rapid change of the distribution function very well. After we march one time step for the BTE, we can obtain the electron density $n_i(x)$ at the $x-$slice on the subband $i$,

$$n_i(x) = \frac{\sqrt{m_{x,i} m_{y,i}}}{2\pi^2\hbar^2} \iint f_i(x, \omega, \theta) d\omega d\theta. \qquad (5)$$

Assuming that the electron probability density is proportional to $|\varphi_i(z;x)|^2$ in the confinement direction, we obtain the electron density $n_i(x, z)$

$$n_i(x,z) = n_i(x)|\varphi_i(z;x)|^2. \qquad (6)$$

Then we sum over all the subbands to get the electron density $n(x, z) = \sum_i n_i(x, z)$. We then plug this $n(x, z)$ into the Poisson equation and solve for a new potential $V(x, z)$. Next, we plug the $V(x, z)$ into the Schrödinger equation at each $x$-slice to obtain new eigen energies $E_i(x)$ and eigen wavefunctions $\varphi_i(z; x)$ to yield a new force $F_i(x)$ and scattering terms for the multi subband BTE of 2D electron gas. This forms a loop. By repeating the loop until the current is converged, we solve the BTE and 2D Poisson equation and 1D Schrödinger equations self-consistently.

Our method includes the acoustic phonon and optical phonon intra-valley scatterings [10]. The 3D$k$ inter-valley scattering parameters can be found in many papers, e.g. [11]. Here we use the parameters from [12] which include three $f$-type and three $g$-type inter-valley scatterings. The 2D$k$ scattering parameters can be derived from the 3D$k$ scattering parameters by calculating

$$I_{ii'}(x) = \int_0^{T_{Si}} \left|\varphi_i(z;x)\varphi'_i(z;x)\right|^2 dz \qquad (7)$$

where $T_{Si}$ is the thickness of the Silicon while the $\varphi_i(z;x)$ and $\varphi_{i'}$ are the $i$-th and the $i'$ subband wavefunctions at $x$ slice respectively.

The boundary conditions of the Poisson equation deserves a short discussion here. Normally, the Dirichlet boundary condition is used for the gate electrodes and the Neumann boundary condition is used for the oxide/air interface. But for the nano-scale MOSFETs, it is pointed out in [3] that the boundary conditions for the Poisson equation at the source/drain contact ends should be the Neumann boundary condition

$$\frac{\partial V(x,y)}{\partial x} = 0 \qquad (8)$$

instead of the standard Dirichlet boundary condition. So the potential at the source/drain contacts could not be equal to the source/drain voltage but float to fulfill the charge neutrality. The floating boundary condition redefines the source/drain contacts; hence we do not need to resolve the complicated coupling between the thin body device and the large source/drain.

When we solve the Poisson equation by using the Newton-Raphson method we need to approximate the term $\frac{\partial n}{\partial V}$. Assuming that the electrons are at equilibrium and obey the Fermi-Dirac distribution, we derive

$$\frac{\partial n}{\partial V} = N_c F_{-1/2}\left((V(x,z) - E_f(x))/V_t\right) \qquad (9)$$

where $V_t = k_B T$ and $V(x, z) - E_f(x)$ are obtained by solving

$$n(x,z) = \frac{1}{V_t} N_c F_{1/2}((V(x,z) - E_f(x))/V_t) \qquad (10)$$

where $N_c$ is the effective density of states in conduction band. $F_s$ is the Fermi-Dirac integral of order $s$. But for the nano-scale MOSFETs, the electrons could be very far away from the equilibrium, especially in the channel. $\frac{\partial n}{\partial V}$ obtained by Eq. (9) should be scaled by a factor to obtain the converged results. We use the factor $0.4$ to obtain the numerical results in this paper.



Authorized licensed use limited to: Peking University. Downloaded on December 17, 2009 at 04:34 from IEEE Xplore. Restrictions apply.

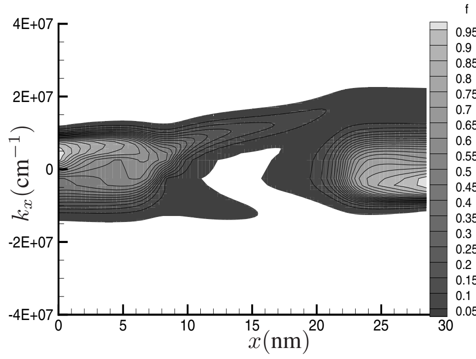


Fig. 3. The first subband distribution $f_1(x, k_x)$ at $V_{GS} = 0.5$V and $V_{DS} =$ 0.6 with scattering. The region with $f_1(x, k_x) < 0.01$ is cut off.

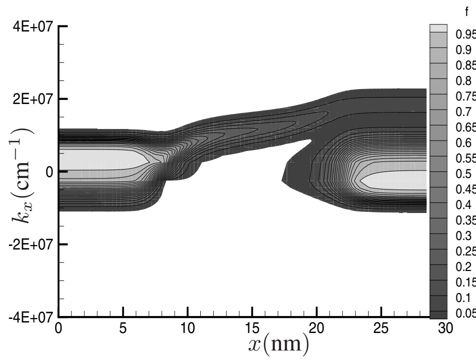


Fig. 4. The first subband distribution $f_1(x, k_x)$ at $V_{GS} = 0.5$V and $V_{DS} =$ 0.6 without scattering. The region with $f_1(x, k_x) < 0.01$ is cut off.

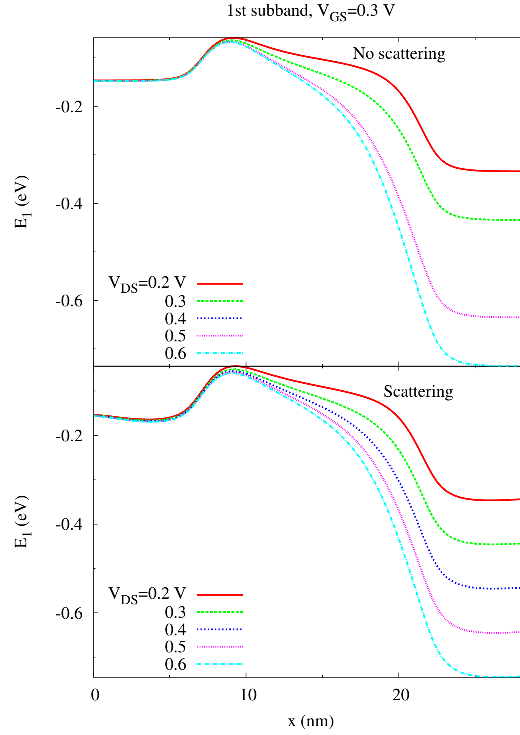


Fig. 5. The first subband at $V_{GS} = 0.3V$ at different $V_{DS}$. The lower one is calculated with scattering, and the upper one is calculated without scattering. For the floating boundary condition is used at the source/drain contact ends, the subbands are almost flat at two ends, especially for the ballistic transport case.

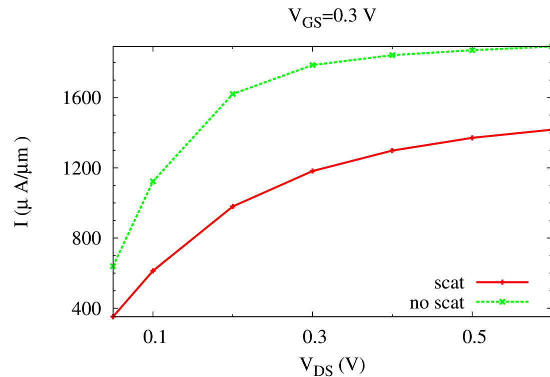


Fig. 6. The $I_{DS} - V_{DS}$ curve at $V_{GS} = 0.3$ V.

## III. Numerical Simulation of a DG MOSFET

We simulate a 9.0 nm gate length DG MOSFET with a body thickness of 3 nm and source/drain doping of $10^{20}$ cm$^{-3}$. The effective oxide thickness (EOT) is 1 nm. And the length of the source/drain is 9.9 nm.

The first subband distribution function with and without scattering at $V_{GS} = 0.6$V and $V_{DS} = 0.6$ V are shown in Fig. 3 and Fig. 4, respectively. Fewer electrons will approach the drain due to scattering.

The first subbands at $V_{GS} = 0.3$ V and $V_{DS} = 0.2, \cdots, 0.6$ V are plotted in Fig. 5.

The $I_{DS} - V_{DS}$ and $I_{DS} - V_{GS}$ curves with and without scattering are compared in Fig. 6 and Fig. 7 respectively. We obtain the current-voltage curve consistent with that of [13]. From the two figures it can be seen that the scattering reduces the current by $20\% - 40\%$.

The potential with scattering at $V_{GS} = 0.3$ V and $V_{DS} =$ 0.6 V is in Fig. 8.

The average velocity along the source-drain direction is in Fig. 9 where the average velocity along the channel with and without scattering are compared at $V_{DS} = 0.05$ V and $V_{DS} =$ 0.6V. From the figure it can be seen that the influence of scattering is obviously both under the low and high lateral



Authorized licensed use limited to: Peking University. Downloaded on December 17, 2009 at 04:34 from IEEE Xplore. Restrictions apply.

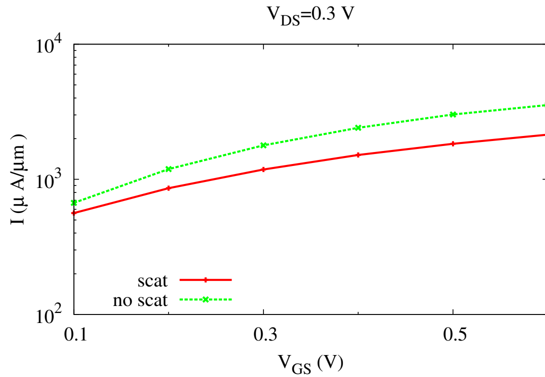


Fig. 7. The $I_{DS} - V_{GS}$ curve at $V_{DS} = 0.3$ V.

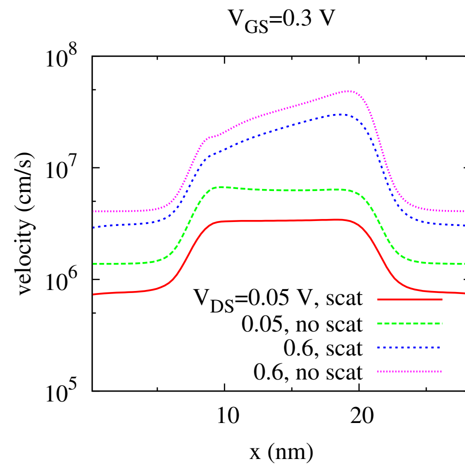


Fig. 9. The average velocity along the source-drain direction. We can see clearly that the scattering reduces the average velocity of the electrons.

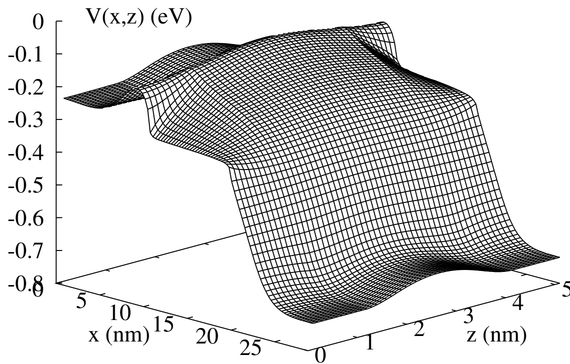


Fig. 8. The potential at $V_{GS} = 0.3$ and $V_{DS} = 0.6$ V

electric fields.

## IV. Conclusions

We presented a deterministic multi-subband simulator of 2D electron gas for the nano-scale ultra-thin double gate MOSFETS. This provides an alternative way to investigate the detail of the nano MOSFETs.

## V. Acknowledgement


This work is supported by the NKBRP (Grant 2006CB302705, 2005CB321704) and the NSFC (Grant 10701005). Haiyan Jiang is also partially supported by the US Army Research Office (Grant No.: W911NF-07-1-0492).


## References


[1] Z. Ren, "Nanoscale MOSFETs: Physics, simulation, and design," Ph.D. dissertation, Purdue University, West Lafayette, IN, 2001.

[2] J. Saint-Martin, A. Bournel, F. Monsef, C. Chassat, and P. Dollfus, "Multi sub-band Monte Carlo simulation of an ultra-thin double gate MOSFET with 2D electron gas," *Semicond. Sci. Technol.*, vol. 21, no. 4, pp. L29–L31, 2006.

[3] Z. Ren, R. Venugopal, S. Goasguen, S. Datta, and M. S. Lundstrom, "nanoMOS 2.5: A two-dimensional simulator for quantum transport in double-gate MOSFETs," *IEEE TRANSACTIONS ON ELECTRON DEVICES*, vol. 50, no. 9, pp. 1914–1924, 2003.

[4] H. FITRIAWAN, M. OGAWA, S. SOUMA, and T. MIYOSHI, "Fullband simulation of nano-scale MOSFETs based on a non-equilibrium Greens function method," *IEICE TRANS. ELECTRON.*, vol. E91C, no. 1, 2008.

[5] M. Galler and F. Schürrer, "A direct multigroup-WENO solver for the 2D non-stationary Boltzmann-Poisson system for GaAs devices: GaAs-MESFET," *Journal of Computational Physics*, vol. 212, no. 2, pp. 778 – 797, 2006. [Online]. Available: http://www.sciencedirect.com/science/article/B6WHY-4H40J1M-3/2/1d06d698f0459ab7c8f8448be4244684

[6] J. A. Carrillo, I. M. Gamba, A. Majorana, and C.-W. Shu, "A weno-solver for the transients of boltzmann-poisson system for semiconductor devices: performance and comparisons with monte carlo methods," *Journal of Computational Physics*, vol. 184, no. 2, pp. 498 – 525, 2003. [Online]. Available: http://www.sciencedirect.com/science/article/B6WHY-47MCFSD-1/2/7a9a40e2578790abaa25878839108553

[7] R. Venugopal, Z. Ren, S. Datta, M. S. Lundstrom, and D. Jovanovic, "Simulating quantum transport in nanoscale transistors: Real versus mode-space approaches," *J. Appl. Phys.*, vol. 92, pp. 3730–3739, 2002.

[8] M. Goano, "Algorithm 745: computation of the complete and incomplete Fermi-Dirac integral," *ACM Transaction of Mathematics Software*, vol. 21, pp. 221 – 232, 1995.

[9] G. Strang, "On the construction and comparison of difference schemes," *SIAM Journal on Numerical Analysis*, vol. 5, no. 3, pp. 506–517, 1968. [Online]. Available: http://link.aip.org/link/?SNA/5/506/1

[10] P. Dollfus, "Si/Si$_{1x}$Ge$_x$ heterostructures: Electron transport and field-effect transistor operation using Monte Carlo simulation," *J. Appl. Phys.*, vol. 82, pp. 3911–3916, 1997.

[11] F. Monsef, P. Dollfus, S. Galdin, and A. Bournel, "First-order intervalley scattering in low-dimensional systems," *Phys. Rev. B*, vol. 65, no. 21, p. 212304, Jun 2002.

[12] S. Smirnov, "Physical modeling of electron transport in strained silicon and silicin-germanium," Ph.D. dissertation, Fakultät für Elektrotechnik und Informationstechnik, von, Wien, Österreich, 2003. [Online]. Available: www.iue.tuwien.ac.at/phd/smirnov/diss.html

[13] J.-H. Rhew, Z. Ren, and M. S. Lundstrom, "A numerical stduy of ballistic transport in a nanoscale MOSFET," *Solid-State Electronics*, vol. 46, pp. 1899–1906, 2002.




Authorized licensed use limited to: Peking University. Downloaded on December 17, 2009 at 04:34 from IEEE Xplore. Restrictions apply.